 doi:10.20944/preprints201908.0230.v1

Article

Investigation of failure mechanism of Lungchok landslide, Sikkim (India)

Neharika Rao Ganta [1*], Neelima Satyam[2]

[1] Research Scholar; shinyneharika65@gmail.com
[2] Associate Professor; neelima.satyam@gmail.com
* Correspondence: shinyneharika65@gmail.com;

Abstract: Globally 30% of landslides occur in the northeastern part of India [1]. One of the major earthquake events in Sikkim, India occurred on 18th September 2011 (Mw 6.9) led to over 300 landslides and 122 human deaths [2]. These landslides not only controlled by natural disasters but initiated due to human activities. The present study considered Lungchok landslide occurred in south district of Sikkim due to 2011 seismic event. The study focused on the failure mechanism of the landslide based on finite element analysis by adopting eight different cases. The deformation characteristic was investigated for dry and saturated slope conditions under static and dynamic behavior considering vehicle loads using GeoStudio software. The FEM analysis has been carried out using load deformation and linear elastic. The analysis shows that the failure of the slope was not sudden due to the 2011 earthquake event, but progressive failure was observed with time and construction activity. The paper demonstrates that, an increase in infrastructure development including construction by hill cutting increased the initiation of landslide with soil erosion. The cracks developed after 2011 earthquake event led to further deformations during future disasters required effective stabilization measures.

Keywords: Finite Element method; Earthquake induced landslide; Static and dynamic analysis; Deformation based failure;

1. Introduction

Landslides are the significant geological hazards observed in mountain regions which lead immense damage to roads, buildings and infrastructure [3, 4]. The mountain area of northeast India covers around 60% of the total area. The landslide's in India prone to 12.6% among which the 5.14% lies in the north-eastern region. It has been noted that the frequency of landslides is increasing in the Himalayan terrain [5]. The landslides vary from north to south and east to west because of climatic condition, seismicity and heavy rainfall.

The two primary mechanisms for landslide occurrences are earthquake and rainfall [6]. Apart from natural disasters, geology and climatic conditions also affect landslide occurrences which have been further intensified due to the increased human activities [7]. Studies show that future incidents of landslides would be triggered more due to human disturbances (land use) rather than climatic changes [8, 9]. Froude and Petley [10], in their study on the global dataset of landslide occurrence showed that 40.2% of landslides caused by construction activity and 11.3 % of landslides are due to illegal hill cutting respectively in between 2004 to 2016. These improper construction activities led to soil creeping downwards and activating fine cracks. The further activation of mass movement is quite common in the Himalayan terrain immediately after the rainy season [11, 12]. These failures are intensified more particularly during the earthquake or after the monsoon season [12, 13]. The landslides after an earthquake event are breeding for future geo hazards and thus further intensified during or after the monsoon season [14]. The soil erosion was observed during earthquake lead to the channel for other hazards, and this cyclic process continues.

 doi:10.20944/preprints201908.0230.v1

The unstable slopes observed during pre-disaster studies need a clear understanding of the problem through visible signs on land [12]. The pre-disaster studies focus on identifying the vulnerable landslide location which helps in post event studies. The post studies signify more on determining the elements that triggered landslides and analyses the stability of slope concerning factor of safety. Many studies have been developed to understand both rainfall and earthquakes induced landslides using finite element method. However, a detailed slope stability analysis is lacking. Several ways are there to compute the slope safety using limit equilibrium methods, kinematic methods including finite and discrete element modelling. The Finite element method (FEM) commonly used for the stability of slopes can be considered with the complex boundary and loading conditions [15]. The stability analysis using the strength reduction technique in FEM was reported by Cai and Ugai [16]. The assessment of pore pressures with infinite slopes was studied by Collins and Znidarcic [17].

In the present study, the failure channel of Lungchok landslide is investigated using pre and post disaster studied using Google images. The downward movement of the slope with the development of cracks was observed. The failure was initiated by several elements with the involvement of external and internal factors. To investigate the disaster chain of Lungchok landslide the work was categorised into pre and post disasters combined with earthquake and rainfall effect along with vehicle loads. The lungchok slope was examined considering eight different cases including dry and saturated condition under static and dynamic loading along with vehicle loads. The present study deals with deformations under numerical simulation by load deformation and linear elastic analysis using the finite element method to identify the possible failure channel of the Lungchok landslide.

2. Details of study area

The September 18th, 2011 earthquake led to reactivation of old landslides and activation of fresh landslides [18]. The present study deals with the newly activated landslide due to the 2011 Sikkim earthquake. The landslide located near Lungchok town at latitude and longitude of $27^0$08'01.88" N, $88^0$23'41.46" E respectively shown in Figure 1. It is situated along the roadway between Lungchok and Singtam villages in the south district of Sikkim state at an elevation of 1686 m above MSL.

Preprints (www.preprints.org) | NOT PEER-REVIEWED | Posted: 22 August 2019 doi:10.20944/preprints201908.0230.v1

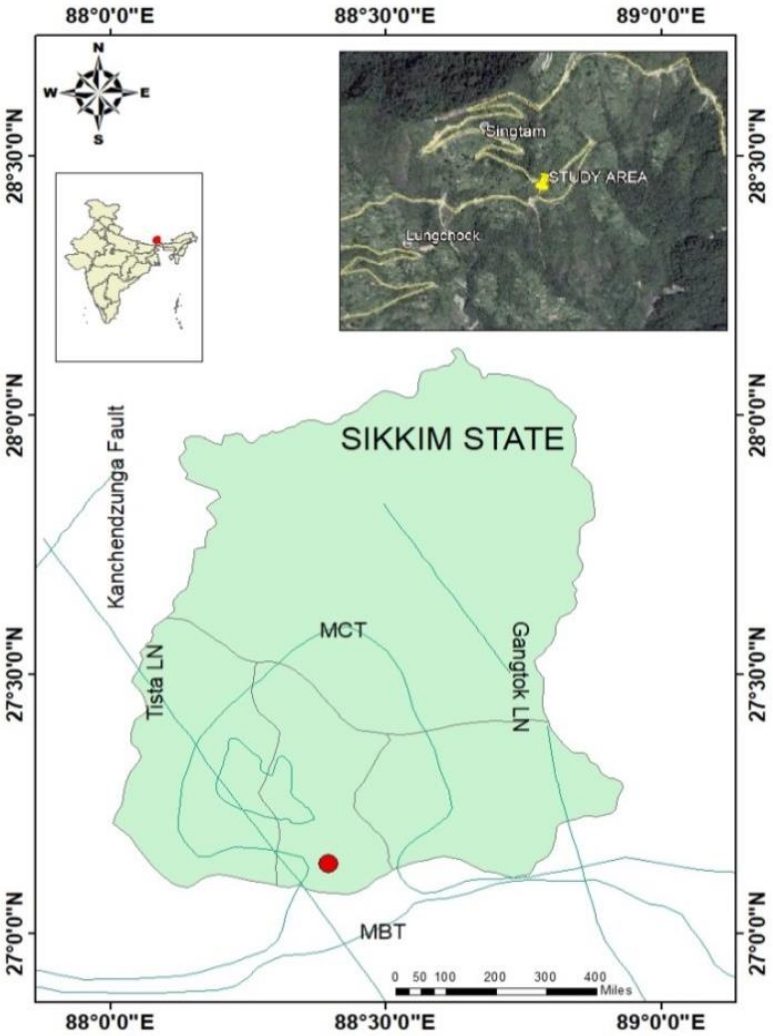

Figure 1. Location of slope considered for the analysis.

The study area is around 73 km from epicentre distance of 2011 event; 16.93 km and 4.02 km away from Main Boundary Thrust (MBT) and Main Central Thrust (MCT) faults respectively. The tectonic collusion and correlation of MBT and MCT is the reason of seismicity in the eastern Himalayan region [19]. The state comprises of slight to moderate earthquakes (Mw 3-6) in the past due to the distribution of MCT, MBT, lineaments and faults. The region comes under seismic zone IV as per Indian standard [20]. The 2011 Sikkim event the moderately high event with a moment magnitude of 6.9 led to 210 landslides including debris, rock slide, and rock fall. The geomorphology and lithology also played an essential role in imitating these landslides during earthquake observed during field study [18]. The frequent landslides are noted in the east and south districts due to the geological covering of Daling group [21]. The south Sikkim is in the physiographic zone of sub Himalayas associated predominantly with phyllite and thinly blended quartzite with surface geology of biotite, tourmaline granite, bouxa dolomite, daling metapelites and Gondwana [22].

The pre-Cambrianmetapelites of Daling group with weathered and fracture rocks accumulate in the southern part of the state [23]. Compared to other districts of Sikkim, the south Sikkim is formed of thin soft slaty half-schistose, and phyllites rocks are highly fragmented [24]. The study area comprises of Gondwana rocks [25]. The moderately steep sloping hill with drained coarse loamy to fine loamy soils of 100cms with greywacke bedrock was observed in the study area [26]. The study area comprises of Gondwana super group with Rangit pebble slate group having

Preprints (www.preprints.org) | NOT PEER-REVIEWED | Posted: 22 August 2019 doi:10.20944/preprints201908.0230.v1

conglomenate, pebble/boulder slate and phyllites according to geological survey of India as shown in the Figure 2.

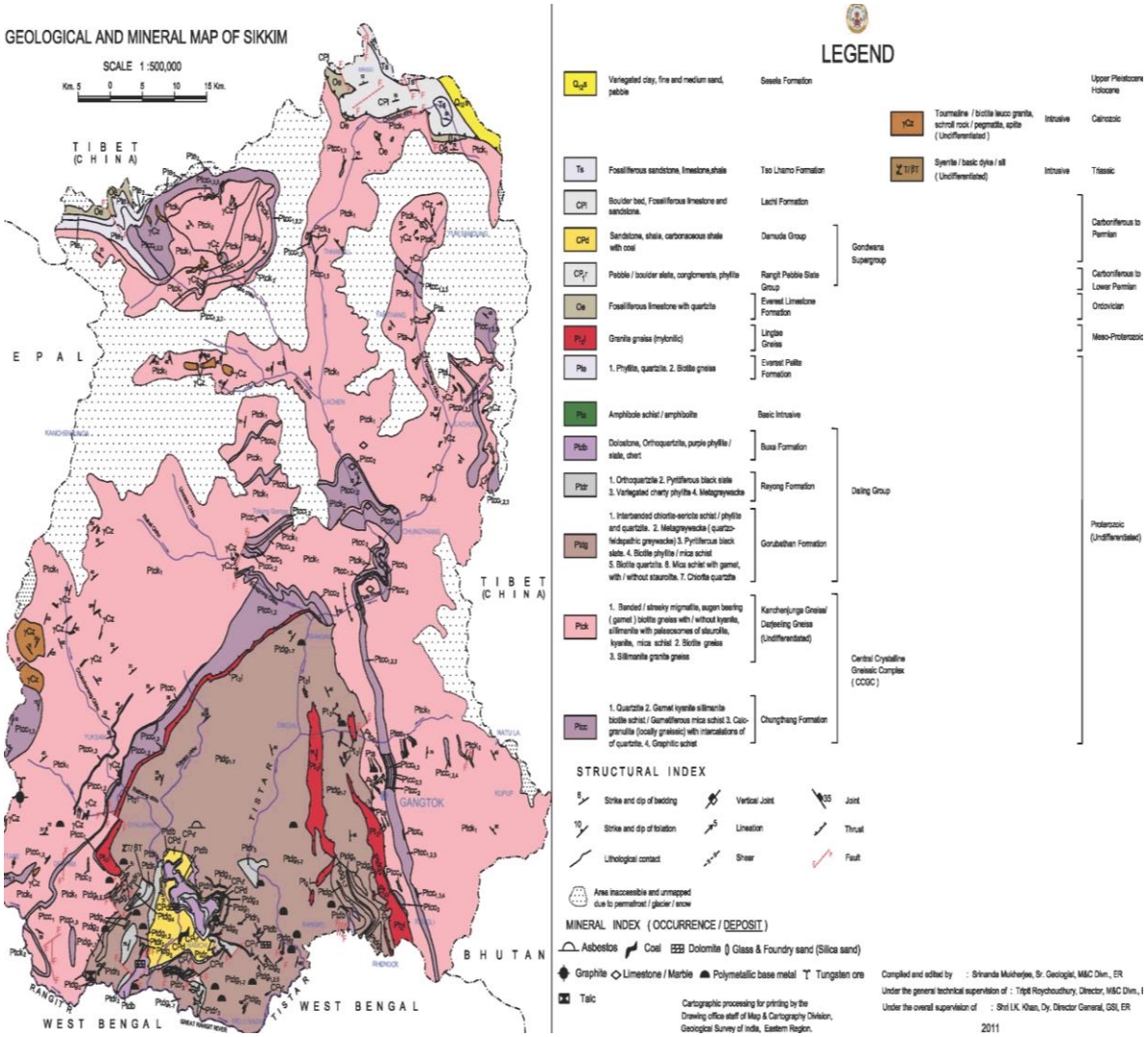

Figure 2. Geology map of Sikkim (Geological survey of India, 2011). http://www.sikenvis.nic.in/Database/GSI_4420.aspx.

From the field observations, the area is covered extensively with thick silty sand with fractured phyllites. The erosion of the soil resulting in landslides is observed in Precambrian rock of phyllites and schist due to its sensitivity and much younger age [18]. The south Sikkim is covered with 2.27 % with the heavily eroded area and 14.33% moderately eroded area. This erosion of soil led to cracks and created channels for infiltration during rainfall. Rainfall increases the pore pressures and responsible for slope failures [27] through infiltration [28].

Increase in rainfall intensity also increases the slope instability by the force of water due to the law of gravity. The rainfall induced landslides are high in the state due to its heavy seasonal precipitation. The central part of the south district receives with more than 2400 mm and adjacent areas with 1200-2400 mm rainfall. The study area receives the mean annual rainfall intensity of 2400-2800 mm [29]. The rainfall has been decreased from nine to five months with an increase in intensity after 2007 [29]. Because of the increase in rainfall intensity slope instability is increasing especially along the road networks mainly due to improper fills and unbalanced excavation during road construction. The vehicle loads further led this soil steeping downwards and developed cracks beneath the road section. Rapid infrastructure development is going due to significant role of transportation plays in the life of people in Sikkim.

 doi:10.20944/preprints201908.0230.v1

3. Data obtained

The Lungchok landslide was identified as a newly initiated landslide occurred during September 2011 earthquake event. The analysis from the aerial photographs during the year 2006-2011 respectively showed that the slide was activated after the 2011 earthquake. From the observation of pre and post Google earth images, the failure was initiated from the past. The Lungchok landslide is of rotational slide led to the blockage of the road as it was built on an unstable slope.

From Google images, it is observed that the roadway was not constructed until the year 2006 shown in Figure 3a. A few years later in 2009, an earthen road 1 and 2 one above the other with an elevation of 0.127 km difference was made on the slope as shown in the Figure 3b. The minor cracks underneath the road one was observed. After a year, the flexible pavement was constructed, and slightly enlarged cracks were found with creeping of soil down towards road two due to the distress of vehicle loads as shown in Figure 3c. The loosen soil abruptly failed when trigged with an earthquake event on September 18th, 2011. The failure slope in between two road section due to the 2011 Sikkim earthquake event is shown in Figure 3d. The rotational failure with deformation extended up to 41.3 m towards the road section 2 and completely damaged. The collapse initiated new cracks of 404 m length with 1.30 m width approximately underneath the road 2.

(a) (b)

Preprints (www.preprints.org) | NOT PEER-REVIEWED | Posted: 22 August 2019 doi:10.20944/preprints201908.0230.v1

(c) (d)

Figure 3. Aerial photographs of the study area: (a) The roadway was not constructed until the year 2006; (b) A few years later in 2009, an earthen road 1 and 2 one above the other was constructed and the minor cracks underneath the road one was observed; (c) After a year in 2010, the flexible pavement was constructed, and slightly enlarged cracks were found with creeping of soil down towards road section two; (d) The failure slope in between two road section during 2011 Sikkim earthquake event.

The basic slope geometry obtained from the Google map is converted and combined with pre and post digital elevation models (DEM). The pre earthquake DEM (August 2011) data obtained through Cartosat-2 from National Remote Sensing Centre (NRSC, Hyderabad). The post-earthquake DEM (2011, October) data collected from the ASTER GLOBAL satellite provided by U.S. Geological Survey (USGS). The contours maps of pre and post satellite data are generated using ArcGIS software. The slope with pre and post earthquake contours shown in Figure 4.

Preprints (www.preprints.org) | NOT PEER-REVIEWED | Posted: 22 August 2019 doi:10.20944/preprints201908.0230.v1

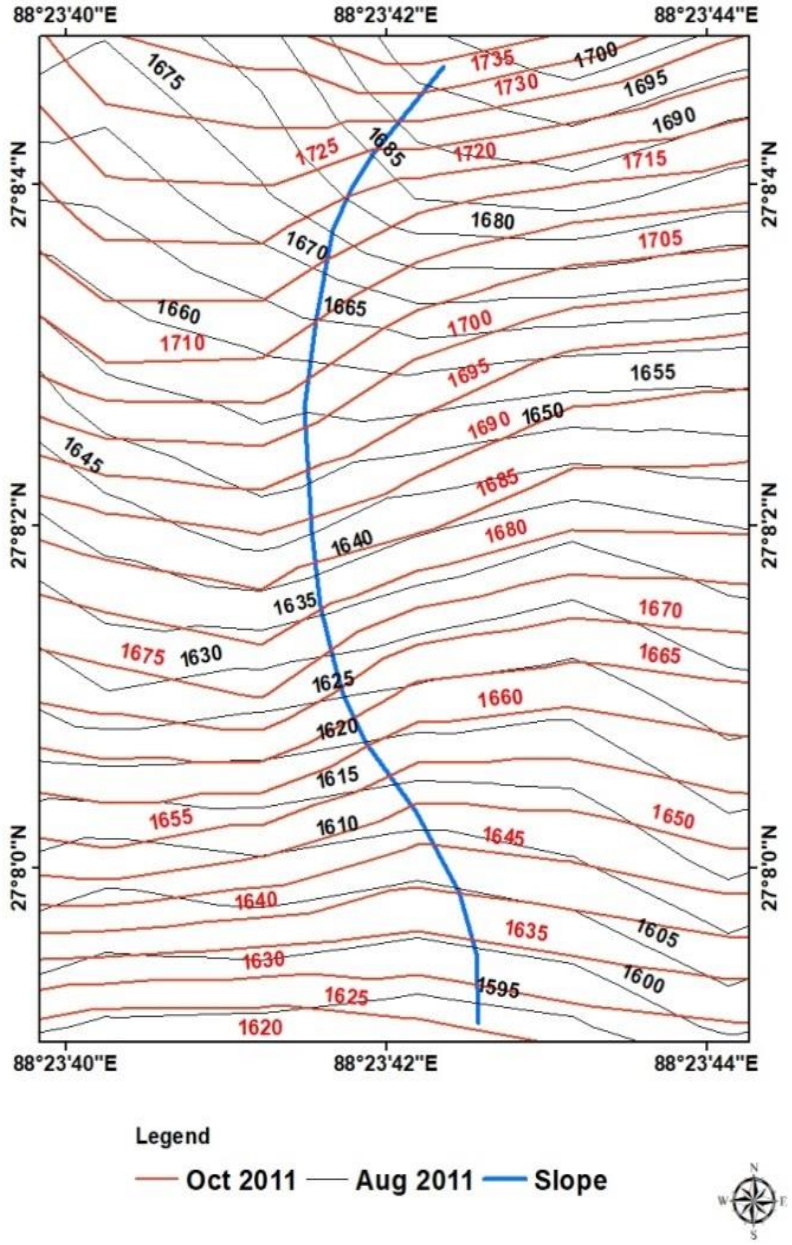

149

150 **Figure 4.** Contour maps of the Lungchok slope (Before and after 2011 Sikkim earthqauke).

151 The ground motion obtained from Gangtok station in three directions but the highest
152 acceleration of 0.156g for the time of 193 sec is considered for the analysis as shown in Figure 5.

Preprints (www.preprints.org) | NOT PEER-REVIEWED | Posted: 22 August 2019 doi:10.20944/preprints201908.0230.v1

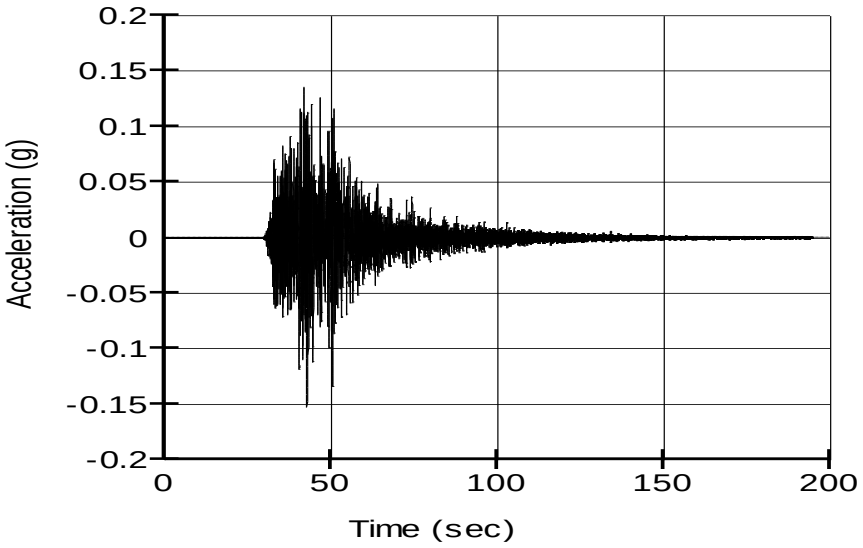

Figure 5. Input Ground motion considered for the analysis (18th September 2011 Sikkim earthquake).

4. Analysis

4.1. Material properties

From the field investigation, the soil is silty sand deposits with the combination of disintegrated soft phyllites. Due to regional meta morphic event the rocks of phyllites and quartzite are partially metamorphized. Thus, when completely weathered shows complex characteristics of meta argillite and meta arenite consist of sandy and fine materials. Therefore, the interbedding of sandy silt, silty sand, silty clay and gravel are characterized and formed as weathered soil. The formation of weathering profile and formation was described by Komoo [30].

The soil samples were collected, and laboratory tests were carried out as shown in Table 1. The slope is considered with two layers for the numerical analysis. Top layer is completely weathered silty phyllites at about 20 m deep and bottom layer consist with partially weathered phyllite rock about 132 m.

Table 1. Geotechnical properties considered for the analysis.

Soil type	Parameters	properties	
		Dry	Saturated
Layer 1: Completely weathered phyllite with silty sand	Unit weight γ (kN/m3)	17.65	20.9
	Youngs modulus E (MPa)	780	480
	Poisson's ratio ν	0.36	0.42
	Elastic Shear Modulus Gmax (MPa)	15.2	9.8
Layer 2: Partially weathered phyllite rock	Unit weight γ (kN/m3)	23.1	25.8
	Youngs modulus E (MPa)	1530	1125
	Poisson's ratio ν	0.30	0.36
	Elastic Shear Modulus Gmax (MPa)	128.8	92.50

4.2. Material properties

The static and dynamic analysis was performed on Lungchok landslide using GeoStudio software. The slope is examined for eight different cases including dry and fully saturated

Preprints (www.preprints.org) | NOT PEER-REVIEWED | Posted: 22 August 2019 doi:10.20944/preprints201908.0230.v1

conditions under static and dynamic loads before and after the construction of the road. Table 2 shows eight different cases considered for the detailed analysis.

Table 2. Cases considered for the analysis.

Case 1	Dry + static + without vehicle loads
Case 2	Dry + static + with vehicle loads
Case 3	Dry + Dynamic + without vehicle loads
Case 4	Dry + Dynamic + with vehicle loads
Case 5	Saturated + static + without vehicle loads
Case 6	Saturated + static + with vehicle loads
Case 7	Saturated + Dynamic + without vehicle loads
Case 8	Saturated + Dynamic + with vehicle loads

The dry slope analysis represents the arid season condition, and fully saturated slope represents the rainfall during monsoon period considering the water table at the surface. The load deformation for static analysis and linear elastic for dynamic analysis were performed using Sigma/w and Quake/w modules of GeoStudio software. In addition to the eight cases considered, the behavior of the dry and saturated slopes due to vehicle loads at time intervals of 1, 6, 12 and 24 months respectively has been evaluated using load deformation analysis. This study was performed to investigate the proper failure channel of the slope under various conditions.

5. Model description

The finite element analysis has been carried out to estimate the deformation of the slope. Finite element approach is widely used due to its connectivity in joint elements [31]. The numerical slope model considered for the analysis is of 280 m distance with elevations at the front and rear edge being 1737 m and 1585 m shown in the Figure 6.

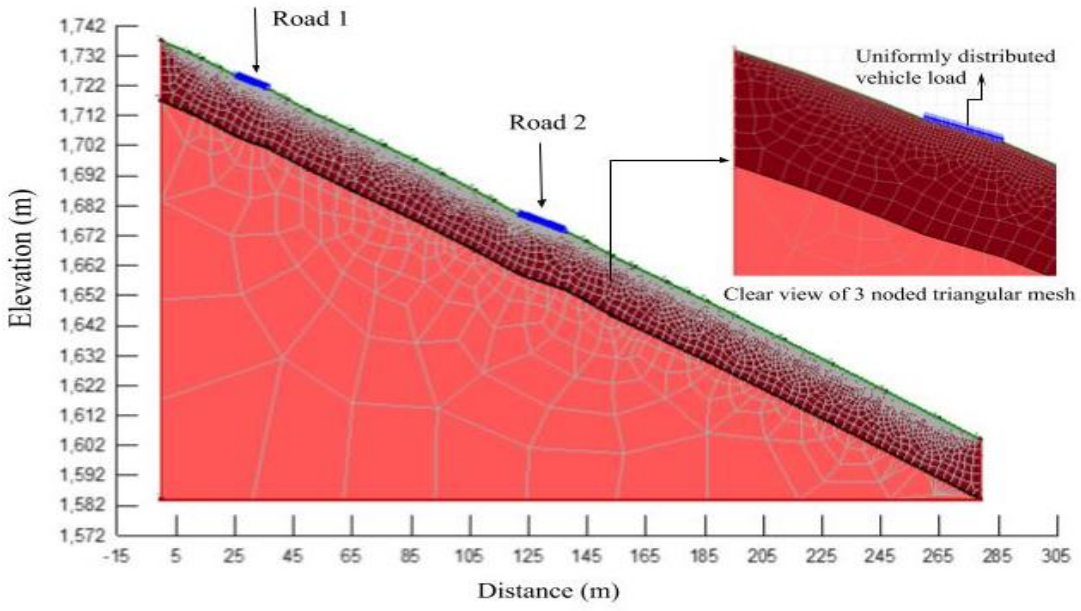

Figure 6. FEM model of slope and clear view of mesh with three node triangular element and vehicle loads at road 1 and 2 sections.

The homogeneous slope considered for the analysis was about 152 m elevation. The triangular plane strain elements having three nodes are used for discretization of elements with a total of 6403 elements thereby considering 6758 nodes for the entire model and discretized with three nodes of triangular elements. The boundary condition along the base of the slope was fixed at X and Y direction, and the elevation of the slope was kept free in the Y direction. The boundary conditions along the slope face were set free in both X and Y directions for determining the displacements. For the dynamic analysis, the input horizontal ground motion along the base of the slope was applied. The vehicle load has been applied uniformly of 392.26kN/m2 as per Indian Road Congress (IRC): 6, 2014 at road 1 and 2.

For the chosen problem the 2D slope was simulated using different modules of GeoStudio software. The deformation under static and dynamic loads of the slope was analyzed using Sigma/W and Quake/W modules. The material model used for the dry slope is carried out using the total stress parameters and for the saturated slope effective drained parameters. The water table has been considered at the top surface to represent a fully saturated condition. The analysis is performed by stage wise by loading and unloading of vehicle loads. The vehicle loads are applied as uniformly distributed loads along the road 1 and 2. The static deformations of the slope were executed under body load without any vehicle loads using In-situ deformation analysis and with vehicle load using load deformation analysis. Similarly, the dynamic deformations of the slope without and with vehicle loads were also considered for detailed analysis using linear elastic.

6. Results and discussion

The static and dynamic analysis for Lungchok slope is performed for dry and saturated slopes under vehicle loads. The variation in horizontal and vertical displacements observed for all the eight cases considered is presented in Table 3.

Table 3. Max horizontal and vertical displacements (m) obtained from the analysis.

Cases considered				Max/Peak horizontal displacement (cm)	Max/Peak Vertical displacement (cm)
Case 1	Dry	static	Without vehicle loads	0.0	0.0
Case 2			With vehicle loads	6.32	16.76
Case 3		dynamic	Without vehicle loads	28.93	0.0007
Case 4			With vehicle loads	28.19	8.54
Case 5	Saturated	static	Without vehicle loads	0.0	0.0
Case 6			With vehicle loads	7.69	22.40
Case 7		dynamic	Without vehicle loads	28.94	0.001
Case 8			With vehicle loads	29.27	11.74

The maximum horizontal displacements of dry and saturated slope for all the eight cases vary from 0 to 28.19 cm and 0 m to 29.27 cm respectively. Similarly, the vertical displacements for dry and saturated slopes are laterally extended from 0 to 8.54 cm and 0 to 11.74 cm. The present study noticed that the deformations were initiated after the application of vehicle loads in both slope conditions by creating rotational failure surface during the application of vehicle loads. The slight increase in deformation was observed further when the water table is considered.

Preprints (www.preprints.org) | NOT PEER-REVIEWED | Posted: 22 August 2019 doi:10.20944/preprints201908.0230.v1

Without the influence of vehicle loads dry and saturated slopes were safe with zero movements. The Horizontal and vertical displacements of both the slopes were increased with the application of vehicle loads were vary from 0 to 6.32 cm and 0 to 22.40 cm as shown in the Figure. 7(a &b). The vehicle loads influenced the vertical deformations compared to horizontal. It clearly shows that the major deformations were increased due to the influence of vehicle loads from zero to 22.40 cm within two years of road construction. Further stability of slope was lowered during heavy monsoon season. The rotational displacements were observed clearly in saturated slope by creating the failure surface underneath road one to two. Thus, create a weak shear zone, and this further degrades due to the percolation of the water into the cracks created by the vehicle loads. Consequently, the stability of soil decreased and failed during the earthquake event.

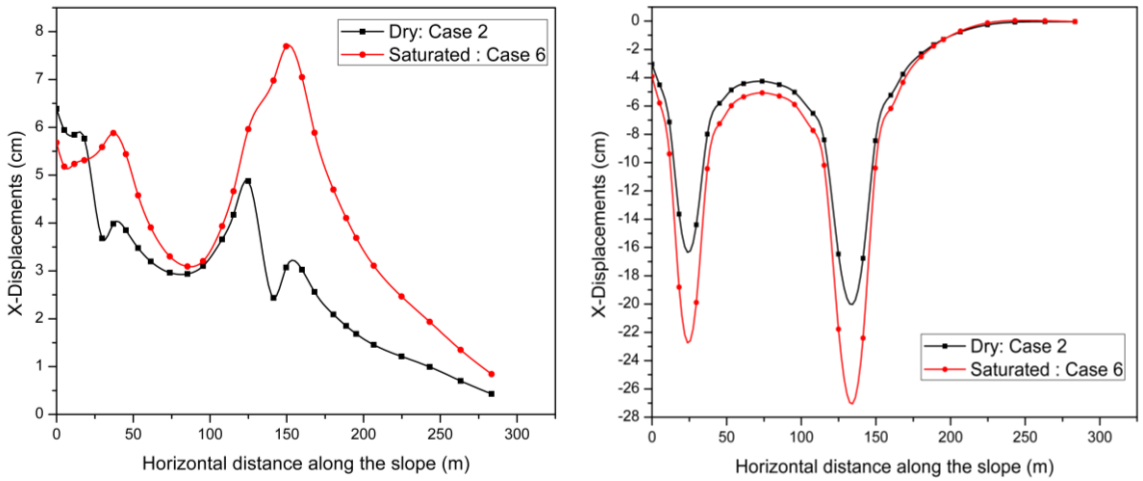

(a) (b)

Figure 7. (a) Horizontal displacements; (b) Vertical displacement of dry and Saturated slope under static loads withvehicle loads.

The rotational failure pattern was not observed both in the dry and saturated slopes when no vehicle loads applied in Figure 8a. The vertical deformations observed are also mostly zero as shown in the Figure 8b. The displacements were gradually increased throughout the slope without any deflation, this failure mostly significant creeping of the soil downwards without creating any failure surface.

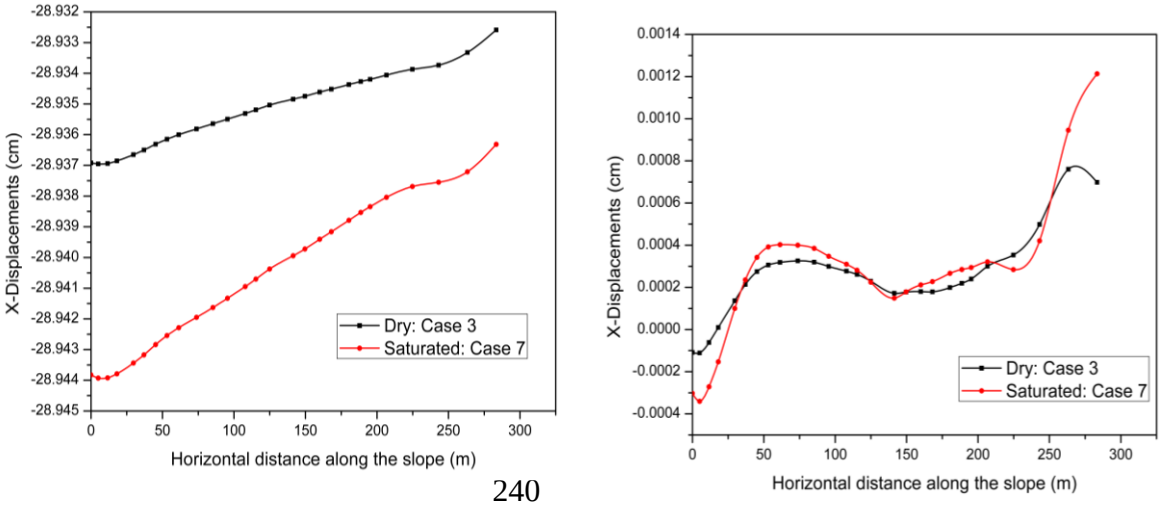

(a) (b)

Preprints (www.preprints.org) | NOT PEER-REVIEWED | Posted: 22 August 2019 doi:10.20944/preprints201908.0230.v1

Figure 8. (a) Horizontal displacements; (b) Vertical displacement of dry and Saturated slope under dynamic loads without vehicle loads.

The failure surface was observed when the vehicle loads were applied under dynamic loading shown in the Figure 9 (a, b). The failure pattern observed clearly in saturated condition is more rotational than the dry condition.

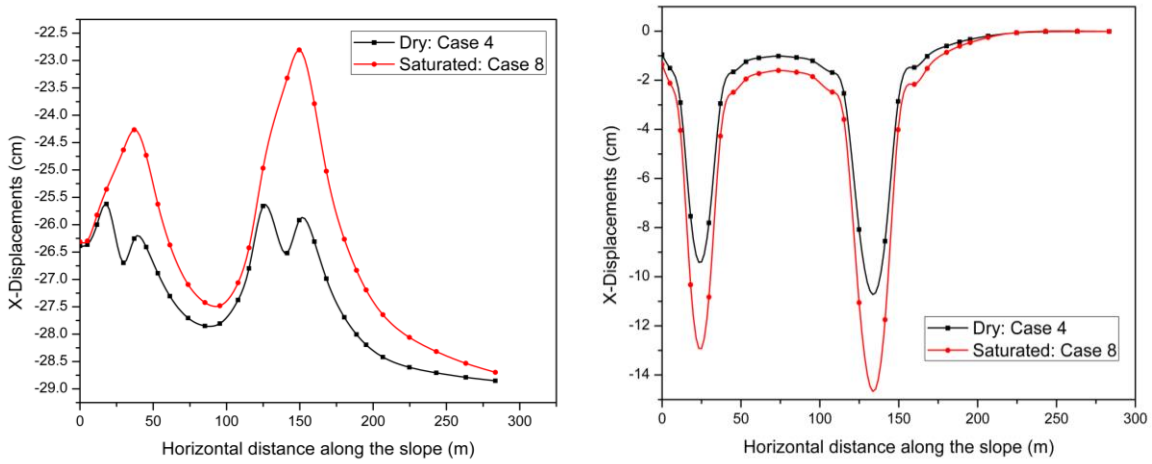

(a) (b)

Figure 9. (a) Horizontal displacements; (b) Vertical displacement of dry and Saturated slope under dynamic loads withvehicle loads.

From all the eight cases observed that, the horizontal displacements in dry and saturated slopes are mostly similar but varied much in vertical displacements due to the influence of vehicle loads. The maximum displacements were observed both in dry and saturated slope under dynamic load along the two road sections with a minute difference in displacements. The vertical and horizontal displacements of the dry and saturated slope are very high in between the two road sections only during the applied vehicle loads. The rotational type of deformation pattern was observed during the application of vehicle loads. The failure observed was identical when cross validated with Google images after 2011 earthquake event.

The behavior of both slopes before the disaster was studied under load deformation analysis at different time intervals of 1, 6, 12 and 24 months shown in the Figure 10(a, b).

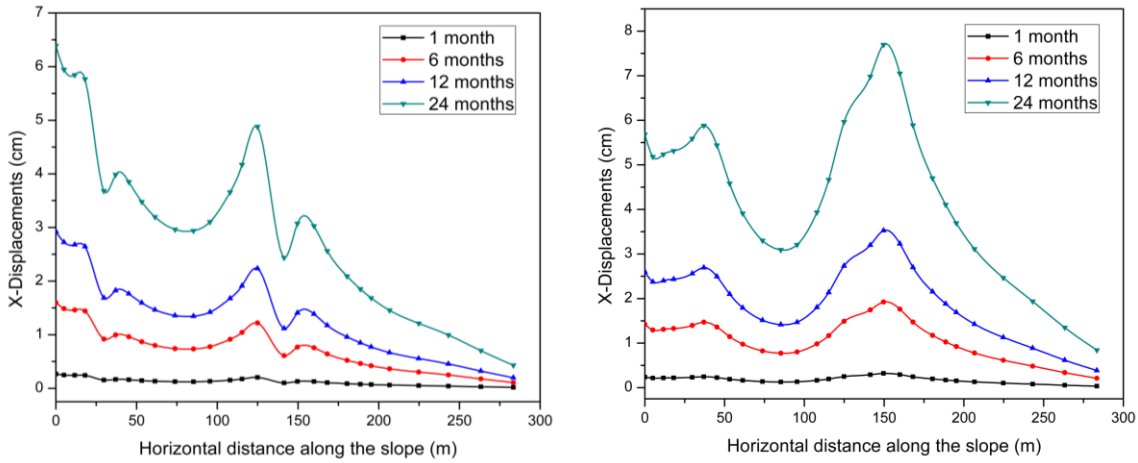

(a) (b)

Figure 10. Horizontal displacements of (a) dry; (b) Saturated slope under dynamic loads with vehicle loads.

The deformations were increased with time in both dry and saturated slope conditions. The deformation of the saturated slope is high when compared to the dry slope. The maximum deformations observed in both slopes are 6.3 cm and 7.69 cm in 24 months. The deformations are gradually increased beneath the road 1 and extended up to road section 2. The deformation obtained due to vehicle loads created cracks beneath the road 1, and this was observed based on the failure in the ground just after the 2011 Sikkim earthquake event as shown in Figure 3c. These cracks further increased during an earthquake event shown in the Figure 3d.

From the results, observed that the failure is not short term, but the preparation process linked with different activities. The deformations were initiated when the additional vehicle load was applied. The results also show that the slope displacements gradually increased with respect time of applied vehicle loads. The failure observed was irrespective to climatic condition but failed was observed more due to vehicle loads. In both slopes models, the displacements are high at the zone of two road sections, and zero deformation at the toe of the slope was observed in each case, and these results are matched with real field scenario.

6. Conclusion

The landslides caused due to human activities are on an increasing trend and are further aggravated due to earthquake and rainfall. The frequent landslides observed in Sikkim (India) are a combination of earthquake, rainfall and anthropogenic activities. The increase in human activity induced landslides can be attributed to the increase in infrastructure development. The present study is based on a finite element model using Lungchok slope located in south Sikkim, India which failed during the September 2011 earthquake event. The pre-disaster slope was modeled under practicable mechanisms to identify the possible failure channel. The conclusions based on the present study as follows:

Two separate conditions of dry and saturated slopes under static and dynamic loadings including vehicle loads based on finite element-based deformation analysis has been performed to understand the proper failure channel. The behavior of slope under vehicle loads from the past two years was studied using load deformation analysis.

The linked progressive failure was observed from the results, and the failure was not sudden due to earthquake event alone. This failure was initiated from the past due to vehicle loads and increased slowly with time creating failure surface. The deformations changed the landscape in the long term creating cracks, erosion and soil creeping was abruptly failed during earthquake effect. Thus, the failure initiated new cracks of 404 m length respectively underneath the road 2.

The various construction activities especially in hilly areas without an adequate measure usually lead to soil erosion and degrading the soil quality along the lines of weakness and thus cause long term failure with additional effects.

From the present study, the Lungchok slope was unstable majorly due to vehicle loads needs continuous monitoring which eventually saves human life.

References

1. 18th September 2011 Sikkim earthquake-Post-Earthquake Reconnaissance Report - West Bengal. https://ndma.gov.in/images/pdf/NDMA_PERT_WB_DraftReport_21December2011_FINAL.pdf.
2. Martha, T.; Govindharaj, K.B.; Vinod, K. Damage and geological assessment of the 18th September 2011 Mw 6.9 earthquake in Sikkim, India using very high-resolution satellite data. Geoscience Frontiers 2015, 6(6), 793-80.
3. Jibson, R.W.; Harp, E.L.; Schulz, W.; Keefer, D.K. Large rock avalanches triggered by the M 7.9 Denali Fault. Alaska Engineering Geology 2006, 83,144-160.
4. Petley, D.N. Global patterns of loss of life from landslides. Geology 2012, 40, 927–930.

5. Gupta,V.; Sah, M.P. Spatial variability of mass movements in the Satluj valley, Himachal Pradesh during 1990-2006. J Mt Sci 2008, 5, 38-51.
6. Keefer, D.K. Landslides caused by earthquakes. Geological Society of America Bulletin 1984, 95, 406–421.
7. Mehrotra, G.S.; Sarkar, S.; Kanungo, D.P.; Mahadevaiah, K. Terrain analysis and spatial assessment of landslide hazards in parts of Sikkim Himalaya. Journal of the Geological Society of India 1996, 47, 491-498.
8. Crozier, M.J. Deciphering the effect of climate change on landslide activity: A review, Geomorphology 2010, 124, 260–267.
9. Anderson, M.G.; Holcombe, E. Community-Based Landslide Risk Reduction: Managing Disasters in Small Steps. World Bank Publications 2013.
10. Froude, M.J.; Petley, D.N. Global fatal landslide occurrence from 2004 to 2016. Natural Hazards and Earth System Sciences 2018, 18, 2161-2181.
11. Paul, S.K.; Bartarya, S.K.; Rautela, P.; Mahajan, A.K. Catastrophic mass movement of 1998 monsoons at Malpa in Kaliganga valley, Kumaon Himalaya (India). Geomorphology 2000, 35, 169-180.
12. Gupta, V.; Mahajan, A.K.; Thakur, V.C.; A study on landslides triggered during Sikkim earthquake of September 18, 2011. Himalayan Geol 2015, 36, 81-90.
13. Tang, C.; Zhu, J.; Qi, X.; Ding, J. Landslides induced by the Wenchuan earthquake and the subsequent strong rainfall event: a case study in the Beichuan area of China. Eng. Geol 2011, 122, 22–33.
14. Pei, L.Z.; Zhou, X.J.; Fang, H. Types, active characteristics and development trend of rainfall-induced landslides after Wenchuan earthquake. Bulletin of Soil and Water Conservation 2012, 32(5), 113–116.
15. Li, G.C.; Desai, C.S. Stress and seepage analysis of earth dams. J GeotechEng 1983, 109, 946–960.
16. Cai, F.; Ugai, K. Numerical analysis of rainfall effects on slope stability. International Journal of Geomechanics 2004, 4(2), 69–78.
17. Collins B D, Znidarcic D (2004) Stability analyses of rainfall induced landslides. Journal of Geotechnical and Geoenvironmental Engineering 130 (4): 362-372.
18. A report on 18th September, 2011 Sikkim earthquake. http://www.sikenvis.nic.in/writereaddata/Earthquake%20induced%20landslides%20in%20the%20Sikkim-Darjeeling%20Himalaya.pdf.
19. Sharma, M.L.; Maheshwari, B.K.; Sinhval, A.; Yogindra Singh. Damage Pattern during Sikkim, India Earthquake of September 18th, 2011. 15th World Conference on Earthquake Engineering 2012, 4087.
20. IS 1893 (Part 1): 2016 Indian Standard Criteria for Earthquake Resistant Design of Structures Part 1 General Provisions and Buildings. Bureau of Indian Standards, New Delhi.
21. Human Vulnerability due to Natural Disasters. http://www.ssdma.nic.in/CMS/GetPdf?MenuContentID=68
22. Nath, S.K.; Raj, A.; Sharma, J.; Thingbaijam, K.K.S et al. Site amplification, qs and source parameterization in Guwahati region from seismic and geotechnical analysis. Seis Res Lett 2008, 79, 526–539.
23. Mehrotra, G.S.; Dharmaraju, R.; Prakash, S. Morphometric appraisal of slope instability of Chilla Landslide, Garhwal Himalaya. Journal of the Geological Society of India 1994, 44(2), 203-211.
24. Sikkim state disaster management plan (2010-2011). http://www.sikkimlrdm.gov.in/downloads/publications/sdmp.pdf
25. Rawat, M.S.; Rawat, B.S.; Joshi, V.; Kimothi, M.M. Statistical analysis of landslide in south district, Sikkim, India: using remote sensing and GIS. Journal of environmental science 2013, 2(3), 47-61.
26. Soils of Sikkim 2007. http://www.sikkimforest.gov.in/soer/Soils%20of%20Sikkim.pdf.
27. Wilson, R.C. Rainstorms, pore pressures and debris flows: a theoretical framework. 2nd edn. Publications of the Inland Geological Society 1989, 101–117.
28. Wieczorek, G.F. Landslide triggering mechanisms special report. National Research Council Washington 1996, 76–90.
29. Sikkim state action plan report. http://dstsikkim.gov.in/Adv/Sikkim%20State%20Action%20Plan%20Report.pdf.
30. Komoo, I. Engineering properties of weathered rock profiles in Peninsular Malaysia. In: Proc. 8th Southeast Asian Geotechnical Conference 1985, 3, 81-86.
31. Troncone, A.; Conte, E.; Donato, A. Two- and three-dimensional numerical analysis of the progressive failure that occurred in an excavation-induced landslide. Eng. Geol 2014, 183, 265-275.